WILEY | Hindawi

*Research Article*

# Apparent Molecular Weight Distributions for Investigating Aging in Polymer-Modified Bitumen

**Miriam Cappello** [ID],[1] **Sara Filippi** [ID],[1] **Yvong Hung,**[2] **Massimo Losa** [ID],[1] **and Giovanni Polacco** [ID][1]

[1]*Department of Civil and Industrial Engineering, University of Pisa, L.go L. Lazzarino, 56122 Pisa, Italy*
[2]*Bitumen Activities, Research Centre of Solaize, TOTAL Marketing Services, 69360 Solaize, France*

Correspondence should be addressed to Miriam Cappello; miriam.cappello@ing.unipi.it
and Giovanni Polacco; giovanni.polacco@unipi.it

The oxidative aging of bituminous binders affects the performance and durability of pavements. In the case of polymer-modified binders, aging involves both bitumen and polymers and has a strong impact on the whole architecture of the material. Rheology may help in understanding these structural changes, and interesting information may be obtained by analysing the evolution of apparent molecular weight distributions. This was demonstrated with a bituminous binder modified with a poly(styrene-butadiene) block copolymer and subjected to prolonged artificial aging. Isothermal frequency sweep tests were used to construct master curves of the phase angle and magnitude of the complex modulus. The master curves were then used to calculate relaxation spectra and apparent molecular weight distributions of the binders, as well as simulated temperature sweep tests. A comparison of the behaviour of the base and modified bitumen highlighted the role of the polymer in aging. Polymer degradation significantly damages the elastomeric network, yet the residual polymer chains still interact with the bitumen molecules and reduce their oxidative aging. The apparent molecular weight distributions were deconvoluted to create an aging index specifically developed for polymer-modified bitumen.

## 1. Introduction

The oxidative aging of bituminous binders has been the subject of several studies and reviews over the last few decades [1–4]. Although the mechanism of aging is extremely complex and involves the entire colloidal structure of bitumen, the main chemical transformations associated with oxidation are the formation of carbonyl compounds (basically ketones) and sulfoxides [5, 6]. One way to quantify aging is thus to use chemical indexes based on the infrared analysis of those functional groups [7–9]. Xu et al. [10] showed the correlation of infrared-derived indexes with mechanical properties such as the complex and Young's modulus. However, despite its popularity, this technique has several limitations as underlined by Marsac et al. [11] who analysed a huge amount of spectra and compared four different calcula-tion methods for the oxidative parameters. The results of the latter study lead to different conclusions depending on the method chosen to calculate the aging indexes. Moreover, the indexes only provide a reliable comparison of the aging when "used on the same type of initial mixture."

Alternative analytical techniques include the determination of the four fractions (saturates, naphthene aromatics, polar aromatics, and asphaltenes) proposed by Corbett [12] and use of X-ray diffraction [13] or gel permeation chromatography (GPC) and nuclear magnetic resonance (NMR) [14]. Another approach is based on performance indexes, thus evaluating the aging in terms of mechanical and rheological properties [15].

Although there are many ways to quantify the level of aging, understanding the mechanism and structural modification of the binders is quite difficult. This is particularly true for

polymer-modified bitumens (PMBs), where the bitumen and the polymer form a complex interpenetrating network and are both affected by aging [16]. Therefore, the literature is mainly focused on the performance [13, 17, 18] or the kinetics of oxidation [19] rather than the mechanisms [20]. With regard to the mechanism, Wang et al. [18] studied the aging kinetic and concluded that the macromolecules gradually degraded into small molecules, thus reducing the integrity of the polymeric network. This network degradation has a direct impact on the overall elasticity and performance of the binder; however, it is not clear how it influences the internal structure. Rheology is thus a powerful technique because it establishes a direct correlation between the structure and properties. This is well known in the case of polymers—see Ferry [21] which is a milestone in this field. Rheology has also been increasingly used in the field of bituminous binders. Today, it is by far the most commonly used technique for their characterization, which can be focused on the performance, but also helps in gaining knowledge regarding the structure and interactions in complex materials such as bituminous binders. The extrapolation of a molecular weight distribution (MWD) from master curves of linear viscoelastic functions is an interesting possibility. The idea of obtaining MWDs using rheological data stems from polymer science [22, 23] and has been extended to bituminous binders [24, 25]. Molecules with a high mobility have a small relaxation time (high-frequency pattern), while molecules of reduced mobility are correlated with lower oscillation frequencies (long relaxation time). This has led to the development of algorithms to calculate an apparent molecular weight distribution (AMWD). The term "apparent" takes into account the fact that mobility and relaxation times are affected by both the real molecular weight and the cohesive energy that derives from Van der Waal's forces between molecules. In other words, this distribution depends on the internal interactions and thus on the molecular structure of the material. The starting dataset can be the master curve of a linear viscoelastic function, as well as a relaxation spectrum [26–28]. In contrast, a technique such as GPC, which evaluates molecular weights in a diluted state, only takes into account the effective dimension of the molecules and is blind with respect to their interactions in the bulk.

Apart from the differing advantages of the two approaches, AMWD intrinsically contains additional information on the internal structure and interactions. However, the absolute values of the AMWD are not reliable which is particularly true for PMBs, where it can assume values that are apparently incompatible with its physical meaning [29]. However, the shape of the distribution and its evolution with aging provide other important information.

The main goal of this work is to analyse this aspect for PMBs obtained using poly(styrene-butadiene) diblock copolymer (SB) and subjected to prolonged artificial aging. AMWD was used to quantify the level of interaction between bitumen and polymers and to define a specific aging index for PMBs.

## 2. Materials and Methods

The PMB was prepared using a base bitumen 70/100 penetration grade, hereafter referred to as B and kindly provided by TOTAL. The base bitumen derives from a vacuum refinery process and has a penetration of 82 dmm (UNI EN 1426) and softening point 50°C (UNI EN 1427). The polymer is SOLPRENE SB (from Dynasol), a poly(styrene)-b-(butadiene) di-block copolymer. The PMB was prepared in 350 ml, aluminium cans. The cans were partially filled with bitumen and heated to 180°C, and then, 5% polymer (by weight of bitumen) and a small quantity (0.1% by weight of bitumen) of sulphur (to avoid phase separation) were added gradually while stirring the system at 5000 rpm using a Silverson L4R for 1 h. The system was then maintained at 180°C for further four hours under gentle stirring (500 rpm). This blending procedure was the result of extensive preliminary testing taking into account both the performance and storage stability of the modified binder.

*2.1. Artificial Aging.* The binders were long-term aged in a pressure aging vessel (PAV). The conventional rolling thin film oven (RTFO) followed by PAV was substituted by a 25-hour PAV of aging as suggested by Lesueur et al. [30]. Extended PAV exposures for 40 and 65 hours were then conducted in the same operating conditions (100°C and air pressure of 2.1 ± 0.1 MPa). Hereafter, the samples are indicated as B (base bitumen) or SB5 (PMB prepared by adding 5% by weight of SB copolymer) followed by the period of PAV aging. For example, SB5 25 indicates the PMB after 25 hours of PAV, while B 65 is the unmodified binder after 65 hours of PAV.

*2.2. Rheology.* Frequency sweep tests were conducted using a Malvern Kinexus PRO Dynamic Shear Rheometer (DSR). Data were collected under isothermal conditions from −10 to +70°C for the base binder and from −10 to +110°C for the PMB. The frequency of small amplitude oscillations varied according to a logarithmic ramping scale from 0.1 to 10 Hz (0.63 to 6.3 rad/s). Depending on the temperature and aging level, parallel plates of 8 and 25 mm were used with gaps of 2 and 1 mm, respectively. Master curves of the phase angle ($\delta$) and magnitude of complex modulus ($|G^*|$) at a reference temperature of 0°C were obtained by applying the time-temperature superposition principle (TTSP) [21]. AMWD and continuous relaxation spectra ($H(\check{\tau})$) were calculated from the master curves. To calculate the apparent molecular weight distribution (AMWD), we used the $\delta$ method as proposed by Themeli et al. [31–33]. The method is based on the idea that oscillation frequencies in master curves are related to molecular weights. This leads to a relation between the phase angle and the cumulative molecular weight distribution (CMWD). The master curve of the phase angle can be transformed into an apparent molecular weight distribution when a correlation between the reduced angular frequency ($\omega_r$) and the molecular weight MW (strictly speaking an apparent MW) is available. In other words, the plot of the master curve of the phase angle as a function of the reduced frequency is directly converted into an apparent molecular weight distribution by applying two transformations. First, the phase angle reported in the y-axis becomes a cumulative apparent weight molecular weight distribution (CAWMWD) through a simple normalization:

$$CAWMWD = \frac{1}{90}\delta. \qquad (1)$$

The reduced angular frequency reported in the $x$-axis then becomes an apparent molecular weight (AMW) using the correlation proposed by Cuciniello et al. [34].

$$\log (MW) = 3.13 - 0.0591 \log (\omega_r). \qquad (2)$$

Finally, the cumulative distribution is converted into the more commonly used weight fraction $(w)$ by differentiation of the CAWMWD with respect to $\log (AMW)$:

$$w(AMW) = \frac{d(CAWMWD)}{d(\log (AMW))}. \qquad (3)$$

The $\delta$ method gives a weight distribution and not a molar distribution. This is why the symbol "$w$" was used in the previous equation and the $y$-axis is labelled as the weight fraction in the AMWD reported in the Results section. To cover the whole range of molecular weights, the master curve must be available in a wide interval of reduced frequencies. In addition, to obtain a smooth distribution from equation (3), the phase angle master curve must also be a smooth material function [29]. Thus, the experimentally derived master curve of the complex modulus was fitted using the 2S2P1D model [35–38]:

$$G^* = G_o + \frac{(|G_\infty| - |G_o|)}{1 + \alpha(i\omega_r\tau)^{-k} + (i\omega_r\tau)^{-h} + (i\omega_r\beta\tau)^{-1}}, \qquad (4)$$

where $G^*$ is the complex modulus, $|G_\infty|$ and $|G_0|$ are the magnitudes of the complex modulus at $\omega_r$ approaching infinity and zero, respectively, $\alpha, \tau, \beta, k,$ and $h$ are model parameters, and $i$ is the imaginary unit. The expression for the phase angle is derived from equation (4) by applying the properties of complex numbers.

The same model is used to calculate the relaxation spectrum with the following approximation [39]:

$$H\left(\check{\tau}\right) = \pm \frac{1}{\pi} \, Im \left[ G^* \left( \frac{1}{\check{\tau} e^{\pm i\pi}} \right) \right], \qquad (5)$$

where $\check{\tau}$ is the relaxation time and Im indicates the imaginary part of the quantity written in square brackets, which is the complex modulus obtained by substituting for $i\omega$, $\check{\tau}^{-1} \exp (\pm i\pi)$, in equation (4).

Multiple stress creep recovery (MSCR) tests were conducted according to AASHTO TP70. The tests were performed at 76°C and consist in 10 creep/recovery cycles with the application of a low stress (0.1 kPa) followed by an additional 10 creep/recovery cycles with the application of a high stress (3.2 kPa).

## 3. Results and Discussion

Frequency sweep data collected in isothermal tests may be combined to build master curves by applying the TTSP. This
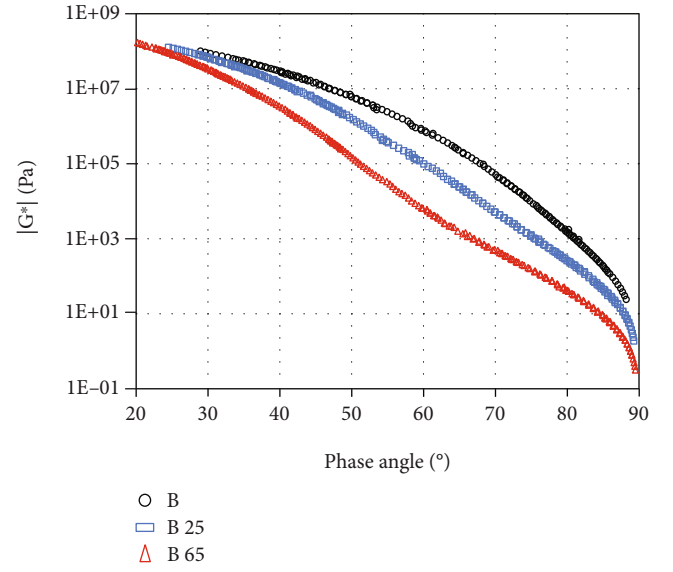


FIGURE 1: Black diagrams for the unmodified binder at different levels of aging.

allows the extrapolation of viscoelastic properties to frequency ranges not accessible experimentally. The applicability of the TTSP in the case of unmodified binders is well accepted and documented [35, 40–42], whereas using the TTSP for PMBs is still an open issue. Cuciniello et al. [43] showed that for bitumens modified with high contents of poly(styrene-butadiene-styrene) block copolymer (SBS), using the TTSP can be difficult especially in unaged binders with a high polymer content due to the integrity of the complex structure formed by the polymeric network which is swollen with bitumen molecules. The polymer has an elastomeric behaviour throughout the entire working temperature range. On the other hand, the bitumen shifts from a Newtonian liquid at relatively high temperatures, to a brittle solid at low temperatures. Therefore, at low temperatures (high frequencies), the bituminous matrix remains rigid, while at intermediate temperatures (frequencies), the two components cooperate with each other. These differences in the temperature susceptibility explain the failure of the TTSP induced by temperature.

Since bituminous binders have a variable composition and likewise the polymers may have differences in molecular weight, composition (styrene/butadiene ratio), and architecture, the TTSP's applicability in PMBs cannot be generalized and each system must be analysed separately. The Black diagram, i.e., the plot of $|G^*|$ versus $\delta$ [17, 42], helps evaluate this applicability. If the isotherms plotted in the $|G^*| - \delta$ plane form a single and continuous curve, then, the TTSP is valid; if not, the TTSP is no longer applicable and there is presumably a modification in the material structure. Figure 1 shows the Black diagrams of B at the aging levels investigated.

Figure 1 demonstrates that the TTSP can be applied in the entire frequency range, irrespective of the degree of aging. In all cases, the isotherms perfectly merge into a single smooth curve. The curves tend to converge at low and high
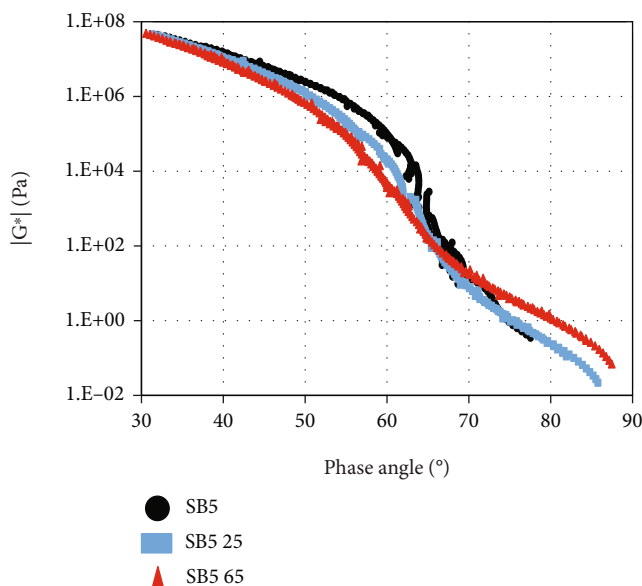
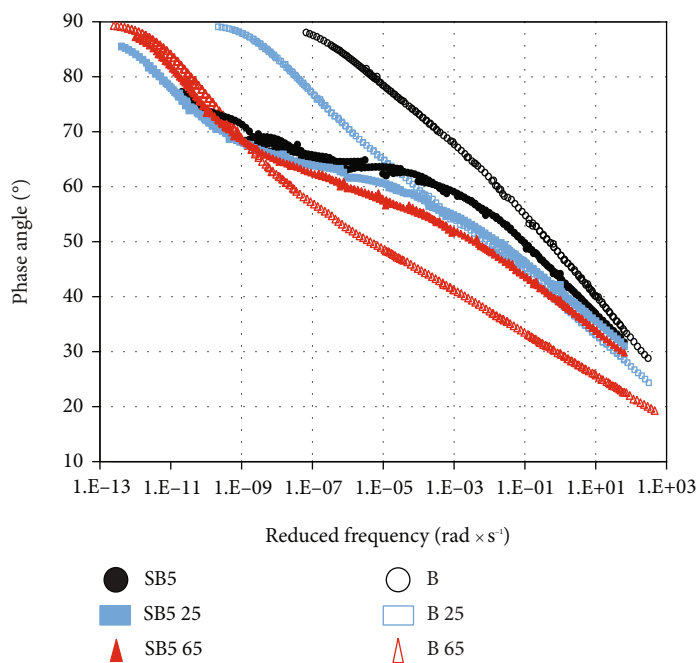Figure 2: Black diagram of SB5 at different levels of aging.



Figure 3: SB5 and B at different levels of aging.

temperatures, but the shape of the curves changes with aging, and differences are well pronounced in the intermediate temperature range. However, the Black diagrams show some limits in the applicability of the TTSP in the presence of the polymer (Figure 2), especially for the unaged binder (SB5) at high temperatures, where the isotherms are not superposed. After 25 hours of aging, the Black diagram presents only a few irregularities and the symptoms of the inapplicability of TTSP disappear after long-term aging. These trends are in accordance with previous observations made with the SBS copolymer [43].

The differences in the Black diagrams with and without polymers are highlighted by comparing Figures 1 and 2. The shape of the Black diagrams suggests that the effect of the polymeric network becomes significant at phase angles of around 55–60°, which are reached with isothermal frequency sweeps conducted above 30°C. Above this temperature, the curves have an inflection point and incongruences appear. At these temperatures, the bitumen alone would be a liquid and the polymer an elastomer. Probably, the increased mobility of the bitumen molecules breaks some of the physical bonds established with the polymer and leads
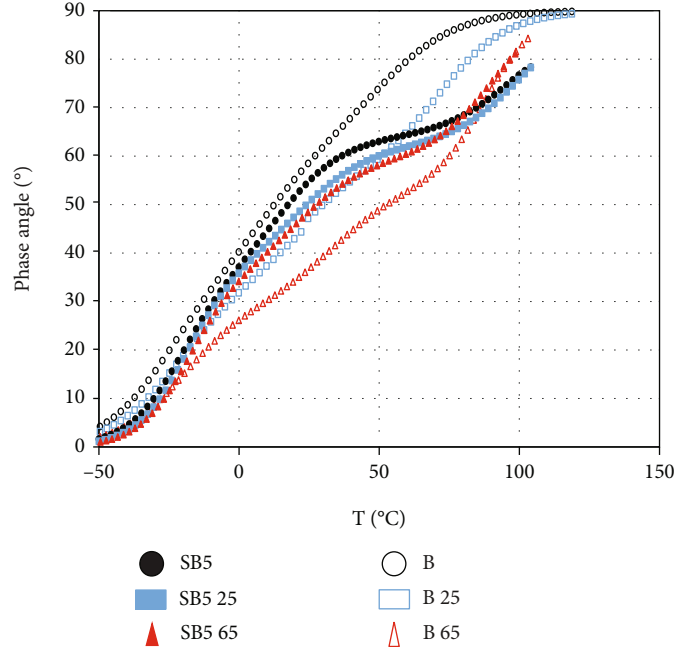
FIGURE 4: Phase angle as a function of temperature after transformation $\omega \longrightarrow T$, $T_r = 0°C$ and $\omega_{test} = 10 \, rad \, s^{-1}$.

to a molecular rearrangement. The fact that, with aging, this structural change seems to disappear may indicate a reduced influence of the polymer on the bitumen structure. This suggests polymer degradation, which is not surprising, since the unsaturated C=C double bonds make it highly sensitive to oxidative phenomena [44, 45]. In other words, unsaturated C=C double bonds along the SB polymer chains are the weak part of the PMB system in the oxidative mechanisms. However, the shape of the Black diagrams also indicates that even at high levels of aging, the behaviour significantly differs from that of an unmodified bitumen. Therefore, there is evidence that the polymer still significantly influences the binder properties. This can be further investigated by looking at the master curves. Building the master curves implies the use of the TTSP, and in the case of unaged SB5, this deserves a clarification. Nevertheless, although a master curve will not necessarily be smooth, it still helps in understanding the evolution of the material with aging. Since the isotherms above 50°C do not superpose completely, the main difficulty is in the shifting method. The horizontal shifting factor is defined as

$$a_T = \frac{\omega_r}{\omega}, \tag{6}$$

where $\omega$ is the angular frequency of individual isothermal measurements and $\omega_r$ is the reduced angular frequency. In the case of bituminous binders, the horizontal shifting factors are well described by the Williams-Landel-Ferry (WLF) equation [21]:

$$\log a_T(T, T_r) = \frac{-c_1(T - T_r)}{c_2 + (T - T_r)}, \tag{7}$$

TABLE 1: Glass transition temperatures from the simulated temperature sweep tests.

| Sample | $T_g$ (°C) |
| --- | --- |
| B | −27.2 |
| B 25 | −22.2 |
| B 65 | −19.3 |
| SB5 | −21.7 |
| SB5 25 | −19.5 |
| SB5 65 | −18.5 |

where $T$ is the test temperature, $T_r$ is the reference temperature, and $C_1$, $C_2$ are the parameters of the WLF model. The building of the master curves agreed with equation (7) for all the binders examined. Figure 3 shows the master curves of the phase angle for the SB5 binder at different levels of aging. For comparison, the graph also contains the master curves of the unmodified binder at the same levels of aging.

These master curves have a "classical" shape. With aging, the curves shift toward lower reduced frequencies and the inflection point is observed at higher phase angles. In contrast, in the SB5 binders, the elastomeric network causes a plateau in the viscoelastic zone. The unaged SB5 has an almost horizontal plateau at a phase angle of about 65 degrees, in the reduced frequency range where the problems with using the TTSP are clearly visible. After 25 hours of PAV, the TTSP works well and the plateau is still evident, though less pronounced. Additional aging leads to a further reduction in the plateau. Comparing the variations in the master curves with and without polymer reveals that aging has a higher impact on the unmodified binder. For example, the reduced frequency corresponding to a phase angle of 55° changes from $3 \cdot 10^{-7}$ to $10^{-1}$ rad·s$^{-1}$, which is about
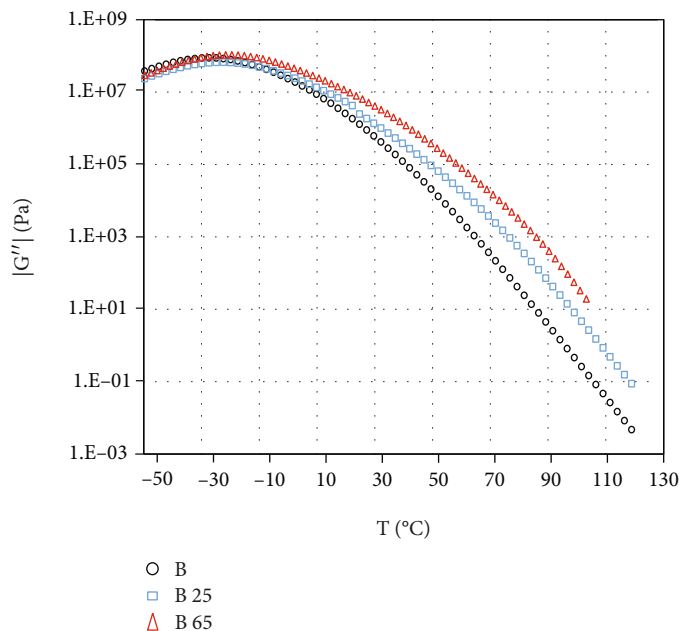
Figure 5: Loss modulus as a function of temperature after transformation $\omega \longrightarrow T$, as in Figure 4.

six orders of magnitude, thus pointing to a strong stiffening of the binder. In contrast, the master curves with the polymer have smaller variations even in the high-frequency range (low temperatures), where the bitumen is assumed to prevail in determining the rheological properties. Therefore, as observed in the Black diagrams, there is evidence of polymer degradation; however, at the same time, the shape of the curves suggests that the polymer-rich phase has a strong influence on the binder properties even at very high levels of aging. In spite of its higher sensitivity to oxidation, the polymeric network somehow continues to do its job. In addition, the polymer seems to inhibit the abovementioned shift in the curves to the left side of the graph. A reduced tendency to aging of PMB has been previously observed by other research groups. Tarsi et al. [46] described that the increase in the complex modulus is lower than with the unmodified bitumens. Sun et al. [18] hypothesized that there might be a mutual protection of bitumen and the polymer. These suggest an antiaging effect exerted by the polymer on the bitumen molecules. There are three possible explanations: (i) the binder modified with the polymer has a much higher viscosity, which inhibits oxygen diffusion during artificial aging in the PAV equipment [47], (ii) the structural rearrangements due to the interactions with the polymer may hide the functional groups more prone to oxidation, and (iii) the polymer may have a "sacrificial" role in the mix if its double bonds preferentially capture the free radicals produced during the oxidative aging.

It is interesting that the master curves of B 65 and SB5 65 converge and superpose in the range of low frequencies (high temperatures). Since the frequency values are not easy to interpret from a practical point of view, a transformation to the temperature domain may be helpful. This can be done using equation (7) and by deriving the temperature as a function of the reduced frequency at a given test frequency
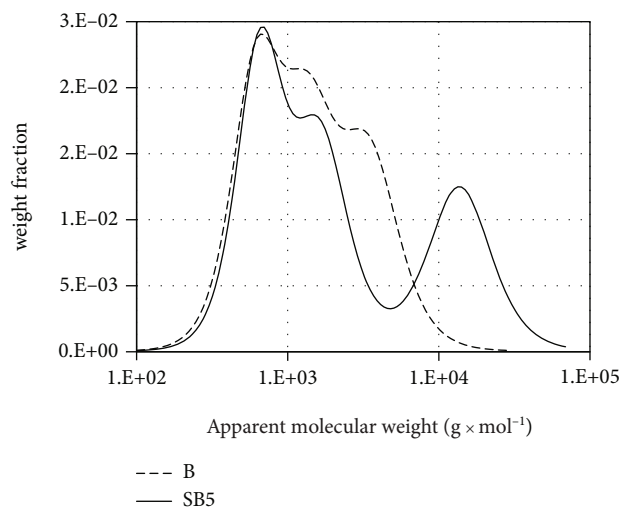


Figure 6: AMWD for the unaged binder, with and without polymer.

$(10 \, \text{rad} \cdot \text{s}^{-1}$ in our case), thus obtaining the representation of a temperature ramp experiment (Figure 4).

All binders except B 65 have very similar phase angles at temperatures below those at which the plateau appears. In contrast, 65 hours of PAV is the only aging level where the unmodified binder merges with the modified one at high temperatures. This representation confirms the moderate effect of aging on the modified binder and shows how the polymer protects the bituminous base from stiffening. Another interesting indication from the transformation to the temperature domain is the apparent glass transition temperature $(T_g)$, which is estimated from the maximum in the loss modulus $(G^")$ master curve (Table 1). Figure 5 shows $G^"$ as a function of temperature for aged and unaged B.
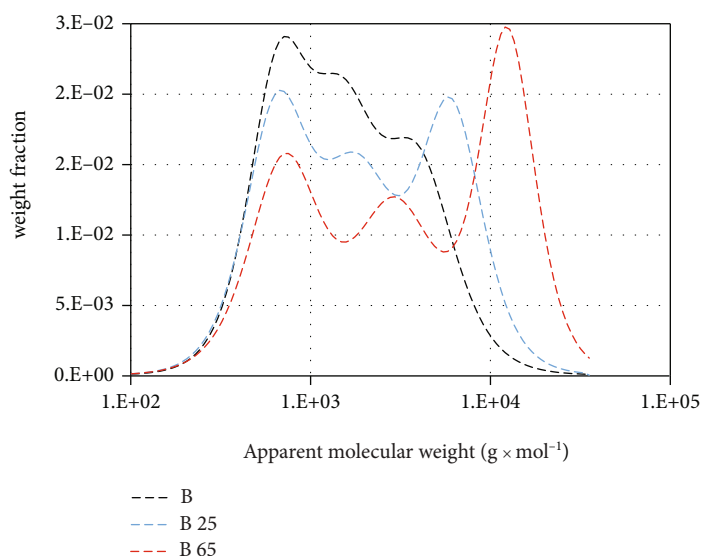
Figure 7: AMWD of B at different levels of aging.

The glass transition temperatures confirm the previous observations. As expected, $T_g$ increases with aging, due to the establishment of new intermolecular bonds that limit the mobility of the binder components. The unmodified binder undergoes a $T_g$ shift of about 8°C with aging, while for SB5, the variation is about 3.2°C. This difference can be due to a lower aging degree of the PMB and/or to the fact that the binder molecules were already limited in mobility due to the bonds with the SB network.

Additional help in understanding the aging sensitivity of bitumen and polymer comes from the $\delta$ method. AMWDs derived from rheological data depend on the interactions among the molecules of the binder and the polymer. The AMWD is thus sensitive to aging, even though the real molecular weight of the molecules does not change significantly. This is particularly important when there is a polymer that creates an elastomeric network able to enclose the bitumen molecules and/or aggregates. To our knowledge, the derivation of apparent distributions in polymer-modified binders has only been shown by Jasso et al. [29], who analysed several binders modified with SBS, which is the most common polymeric modifier. However, the results described for SBS are not limited to that for polymer and can easily be extended to other polymeric modifiers. Jasso et al. showed that in the intermediate frequency range, the phase angle master curve of PMBs may show a minimum. In the $\delta$ method, this implies the appearance of a negative peak in the AMWD. Of course, this makes no sense in the classical interpretation of a molecular weight distribution and this example helps in understanding the real meaning of AMWD. In the case of the master curves shown in Figure 3, there are no local minima in the phase angle. The plateau region corresponds to a minimum in the distribution, and the more the plateau approaches horizontality, the more the weight fractions tend to become zero. Figure 6 compares the AMWDs obtained for the same binder with and without polymer
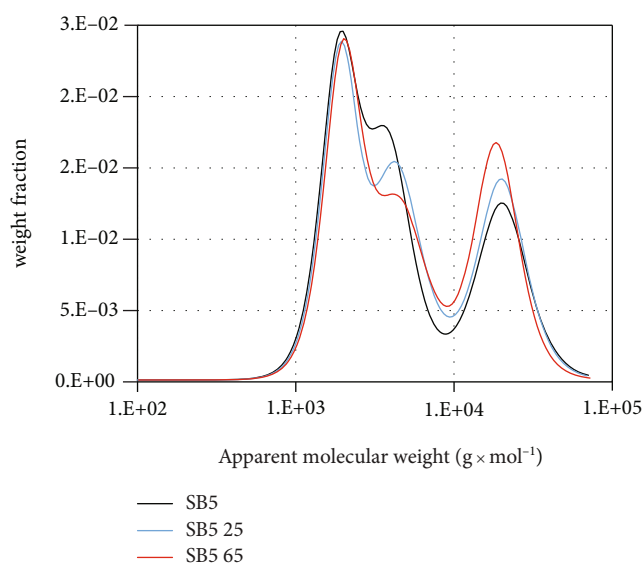


Figure 8: AMWD of SB5 at different levels of aging.

which thus helps to highlight the presence of the polymer (Figure 6).

The minimum due to the plateau zone is clearly visible at apparent molecular weights between 3000 and 8000 g·mol$^{-1}$ for the SB5 binder. The polymeric network establishes secondary bonds with the bitumen molecules and reduces their mobility thus changing the temperature at which they have a liquid behaviour. The $\delta$ method interprets this reduced mobility as an increase in high-apparent molecular weight fractions. The PMB structure is composed of polymer-rich and asphaltene-rich domains that may have different morphologies, depending on the degree of polymer-bitumen compatibility and intermolecular interactions [16]. The peak on the right-hand side of the graph is due to the polymer-rich phase. The intensity and position of this peak are an indicator of the interactions between polymer and bitumen.

TABLE 2: Average apparent molecular weight, dispersion index, and corresponding aging indexes for B and SB5 at different levels of aging.

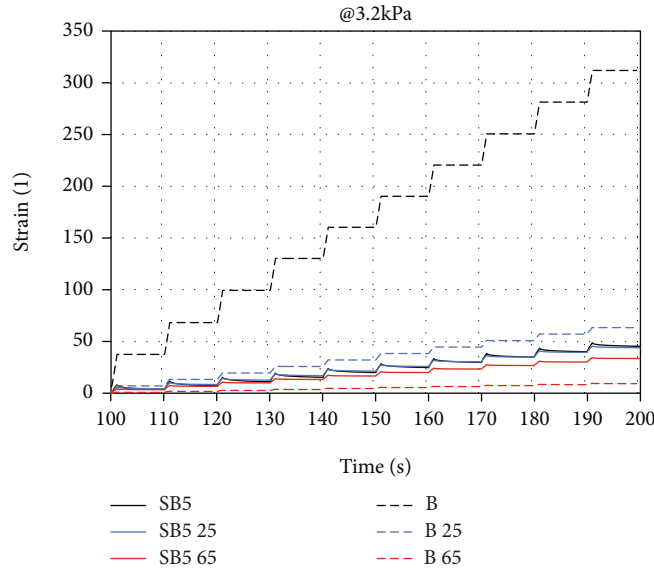| Sample | $AM_w$ | $AI_{Mw}$ | $AM_n$ | $AI_{Mn}$ | DI | $AI_{DI}$ |
|--------|--------|-----------|--------|-----------|------|-----------|
| B | 1362 | 1.00 | 1227 | 1.00 | 1.11 | 1.00 |
| B 25 | 1836 | 1.35 | 1588 | 1.29 | 1.16 | 1.04 |
| B 65 | 2910 | 2.14 | 2356 | 1.92 | 1.24 | 1.11 |
| SB5 | 2124 | 1.00 | 1706 | 1.00 | 1.25 | 1.00 |
| SB5 25 | 2427 | 1.14 | 1943 | 1.14 | 1.25 | 1.00 |
| SB5 65 | 2416 | 1.14 | 1946 | 1.14 | 1.24 | 1.00 |



FIGURE 9: Accumulated strain as a function of time (@3.2 kPa) for B and SB5 at different aging levels.

Unlike what happens at high MW, the AMWDs with and without polymer are almost superimposable at low MW. This indicates that the smallest and the least polar bitumen molecules do not interact significantly with the polymer or at least not enough to shift their relaxation time.

In light of this premise, we can compare the evolution of the AMWD with aging for the two binders. Figure 7 shows the three distributions for the unmodified binder. The curves change significantly due to aging. There is a shift toward higher molecular weights of the right part of the distribution and a much smaller shift on the left side. Therefore, the overall effect is a substantial increase in the dispersion index (DI):

$$DI = \frac{AM_w}{AM_n}, \tag{8}$$

where $AM_n$ is the apparent number-average molecular weight and $AM_w$ is the apparent weight-average molecular weight. These two average values are derived from the apparent molecular weight distributions after discretization into a finite number of intervals:

$$AM_n = \frac{1}{\sum(w_i/AM_i)},$$
$$AM_w = \sum w_i AM_i, \tag{9}$$

where the subscript $i$ refers to the discretization interval. This widening of the distribution leads to a better separation of the peaks. The intensity of the low MW peak diminishes, in favour of higher MW. Since the oxidation does not impact considerably on the real dimension of the molecules, but affects their polarity, the observed variations are thus likely to be mainly due to aggregation of the molecules.

Figure 8 is similar to Figure 7 and shows the AMWDs for the PMBs. The evolution of the distributions with aging is completely different from what was observed for the unmodified binder. Aging changes the distributions more in a vertical direction than in the horizontal one. The curves do not show significant shifts toward a higher molecular weight. The peak at high MW increases in intensity but does not move to higher MW, though it may move a little bit toward the left side of the graph. Moreover, the low MW peak seems to remain almost unperturbed by aging.
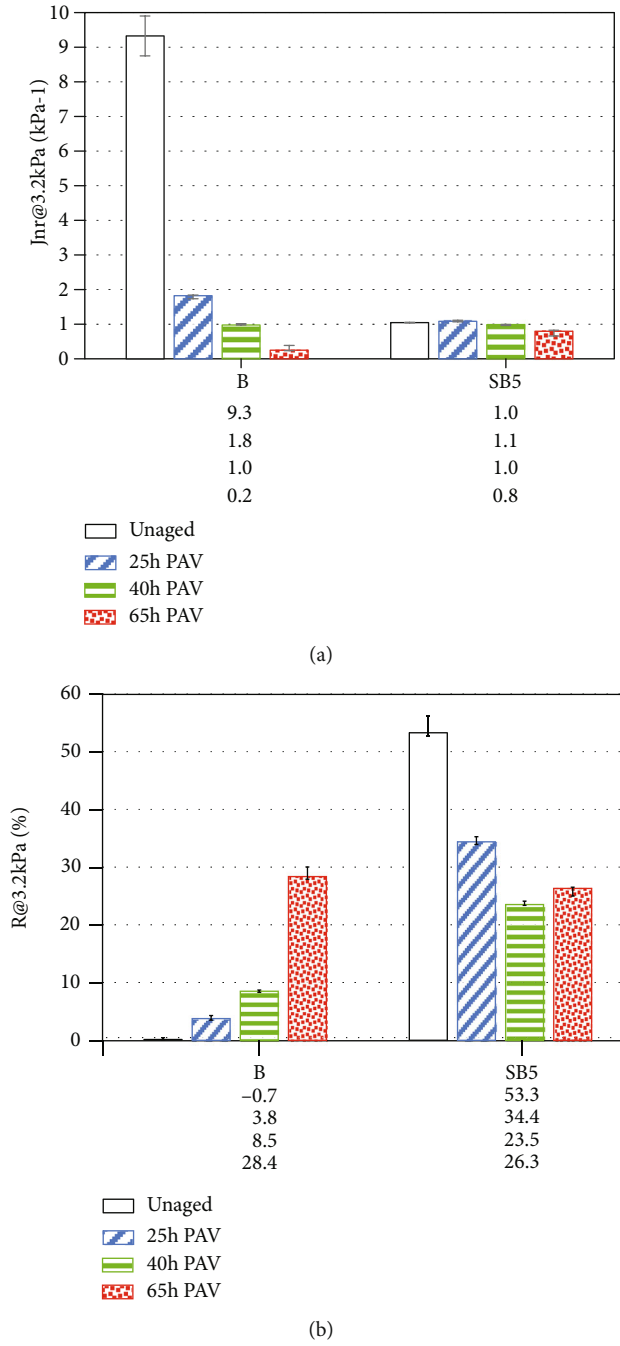
(a)



(b)

FIGURE 10: $J_{nr}$ (a) and $R$ (b) @3.2 kPa. AASHTO M 332 traffic designation: $S$: standard ($J_{nr}$ max = 4.5 kPa$^{-1}$); H: heavy ($J_{nr}$ max = 2 kPa$^{-1}$); V: very heavy ($J_{nr}$ max = 1 kPa$^{-1}$); E: extremely heavy ($J_{nr}$ max = 0.5 kPa$^{-1}$).

Table 2 reports a few data extrapolated from these AMWDs, together with the corresponding aging indexes defined as follows:

$$AI_{Mn} = \frac{AM_{n,a}}{AM_{n,u}}, \tag{10}$$

$$AI_{Mw} = \frac{AM_{w,a}}{AM_{w,u}}, \tag{11}$$

$$AI_{DI} = \frac{DI_a}{DI_u}, \tag{12}$$

where the subscripts "$a$" and "$u$" refer to aged and unaged, respectively.

What is qualitatively described in Figures 7 and 8 is quantified in Table 2. The "horizontal" shift of the AMWD of the unmodified binder leads to notable variations in the average molecular weights and thus in the corresponding aging indexes. In contrast, the "vertical" shift of the PMB gives barely noticeable variations in the same parameters.
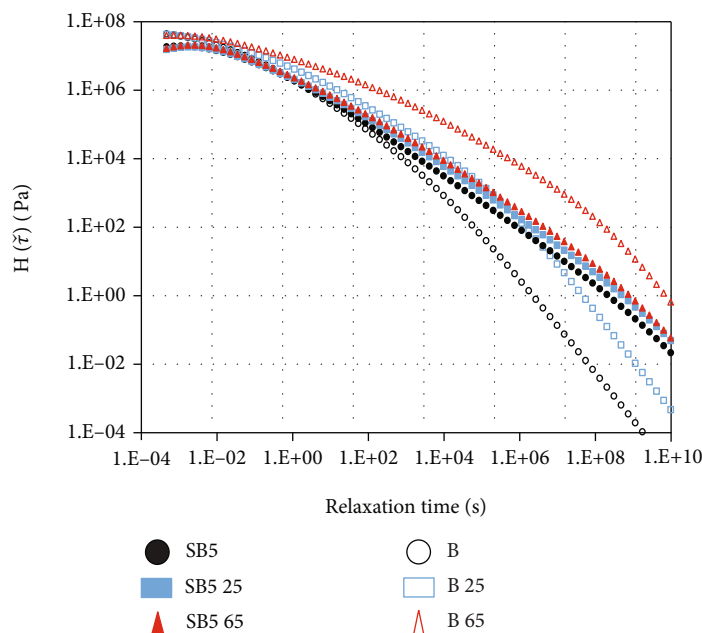
FIGURE 11: Relaxation spectra for the two binders at different levels of aging.

The aging indexes defined in equations (10)–(12) are thus not appropriate for the modified binder. This highlights that the choice of aging indexes must take into account the kind of binder and the specific properties to be evaluated. There has been a recent debate on this issue [48–51].

How can these distributions be interpreted in terms of aging and the internal structure of the binder? On the one hand, there is clear evidence that the polymer undergoes degradation, since the viscoelastic plateau in the phase angle master curve almost disappears with aging. On the other hand, SB5 is still different from B, even at high levels of aging. Therefore, the polymer is still present and able to influence the overall mechanical properties. This is also confirmed by the MSCR test. Figure 9 reports the variation in the measured strain as a function of time for the ten cycles conducted at the higher stress (3.2 kPa). In the case of the base binder, the lower the aging time, the higher the accumulated final strain, as the effect of aging is very pronounced. This confirms the hardening effect of the oxidative reactions occurring during aging. SB5 shows a similar trend; however, the accumulated final strain at unaged conditions is six times lower than B, as typically observed in a PMB.

The variation in the final strain with aging depends on both the contributions of polymer and bitumen phases at the testing temperature. The mechanism could be explained by considering the nonrecoverable compliance ($J_{nr}$) and the percentage recovery ($R$). The first is related to the binder resistance to accumulating permanent deformation and is considered as an indicator of the bitumen hardening. The percentage recovery gives information on the polymer degradation and is representative of the quality of the modification and integrity of the polymer network [52–54]. Figure 10 reports $J_{nr}$ and $R$ at a stress level of 3.2 kPa. The binder B shows a significant variation in $J_{nr}$. This sample has a *standard* traffic designation under unaged conditions

but becomes *very heavy* after 25 and 40 h of aging, and *extremely heavy* after 65 h. In contrast, SB5 unaged shows a $J_{nr}$ around 1.0 kPa$^{-1}$ which is the limit between *heavy* and *very heavy* as traffic designation and remains with the same designation even after 65 h of aging.

In the case of unmodified bitumen, $R$ increases with aging due to the bitumen hardening, which leads to a reduction in the creep portion of the strain. In contrast, SB5 has a higher unaged value (53.3%), which decreases due to polymer network degradation (23.5% after 40 h of aging) thus indicating that the PMB response is controlled by the polymeric phase. However, after 65 h of aging, there is an inversion and the $R$ value increases. The polymeric chain has already achieved a high level of degradation and the binder response is now controlled by the hardened bituminous matrix.

This is in line with the hypothesized sacrificial degradation of the polymer that protects the bitumen molecules. If this degradation mainly consists of chain breaking, the effect is a consistent reduction in the average molecular weight of the chains. This leads to a weakening of the elastomeric network, which probably splits into smaller clusters with reduced elasticity but is still able to interact with the bituminous molecules. Therefore, although the elastomeric properties of the binder are reduced considerably by the chain degradation, the mobility of the bitumen molecules does not change much. For this reason, the appearance of new polar groups due to oxidation is partially hidden in the AMWD by the higher degree of aggregation still induced by the polymer. The overall effect is a depletion of the elastomeric behaviour, without significant gains in internal motion. The AMWD curve thus evolves "vertically" instead of horizontally in the presence of the polymer. For the same reason, the relaxation spectrum is highly sensitive to aging for the B binder, but only moderately for SB5 (Figure 11). Its use in characterizing aging therefore remains useful for
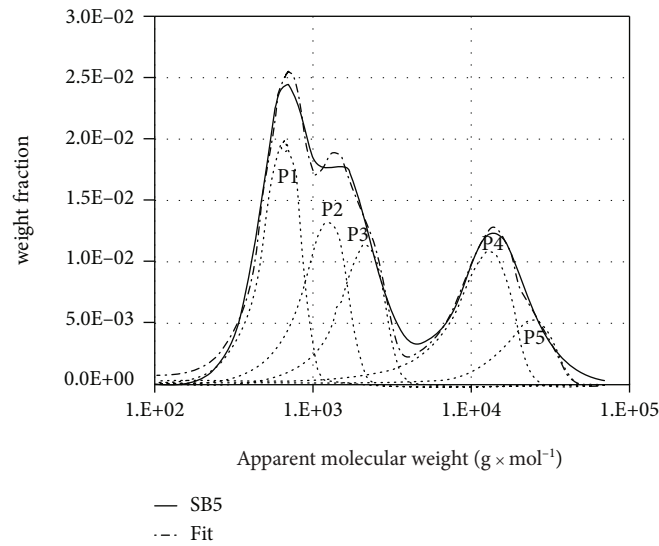
FIGURE 12: Deconvolution in five Gaussian peaks of the AMWD for SB5 binder.

unmodified binders [26, 55–57] but seems inadequate for the PMBs.

For an appropriate aging index for the PMB, the relative quantity of the low- and high-molecular weight parts of the distribution can be helpful. The two areas can be easily calculated with a deconvolution procedure. In this case, the use of five Gaussian peaks gives a good fit of the AMWD (Figure 12). The low ($P_L$) and high ($P_H$) molecular weight populations can then be obtained as

$$P_L = \frac{A_1 + A_2 + A_3}{A_{\text{tot}}}, \qquad (13)$$

$$P_H = \frac{A_4 + A_5}{A_{\text{tot}}}, \qquad (14)$$

where $A$ is the area of the peak and tot indicates the area of the whole AMWD. The results are reported in Table 3, together with an aging index defined as

$$\text{AI}_1 = \frac{(P_H/P_L)_a}{(P_H/P_L)_u}. \qquad (15)$$

Equations (13) and (14) were used because the deconvolution peaks associate the $P_H$ and $P_L$ values with the molecules that belong or not to the polymeric network, respectively. Of course, other criteria can be adopted, for example, by dividing the distribution into two zones. In this case, the apparent distribution corresponding to the local minimum would probably be the most appropriate value to cut the distribution in two (left and right) subsections. This would give slightly different numerical values, without affecting the above-reported considerations.

Moreover, equations (13) and (14) are limited to those cases where the high-molecular weight peaks are clearly detectable. This means that the equations must be considered as being specifically formulated for the AMWD where the two peaks derive from the plateau zone, which is always

TABLE 3: Data for SB5 at different levels of aging.

| Sample | $P_L$ | $P_H$ | $P_H/P_L$ | $\text{AI}_1$ |
| --- | --- | --- | --- | --- |
| | Area (%) | Area (%) | | |
| SB5 | 66.8 | 33.2 | 0.50 | 1.00 |
| SB5 25 | 64.0 | 36.0 | 0.56 | 1.13 |
| SB5 65 | 60.8 | 39.2 | 0.64 | 1.30 |

well visible in the rheological characterization. In contrast, due to the use of solvents, in a GPC distribution, the polymeric network is no longer present and the method is not applicable.

## 4. Conclusion

Studying the rheological properties of bituminous binders is an effective way to characterize the evolution of the performance of the binders as a consequence of artificial aging. In the case of polymer-modified binders, both the bitumen and the polymer are subject to oxidation and the overall behaviour is the result of a complex mechanism where the two contributions are not easily distinguishable.

However, a comparison of the variation of the phase angle master curve with aging in the two binder types provides insights into this mechanism. In the case of the SB copolymer, it seems that the polymer slows down the aging of the binder, through a sort of sacrificial effect. The higher sensitivity of SB to oxidation derives from its high content of unsaturated carbon-carbon double bonds, whose presence may induce chain breaking. Even a small number of breaks considerably reduces the average molecular weight and strongly influences the polymeric network. This leads to a substantial alteration in the horizontal plateau which is only clear in the master curve of the unaged PMB. In other words, the PMB master curves corresponding to different levels of

aging have considerable differences in the shape but remain quite close on the oscillation frequency axis.

In contrast, the unmodified binder basically maintains the shape of the master curves but shows an increase in stiffness, highlighted by a marked shift in the reduced frequency axis. This means that, although reduced in length, in the PMBs, the polymer macromolecules maintain their chemical structure and thus the ability to interact with some bitumen molecules.

These interactions are responsible for a scarce reactivity with oxygen and explain the small shift in the reduced frequency with aging. Moreover, the interactions between the polymer chains and bitumen molecules strongly limit the mobility of the latter. This effect can be noticed when a frequency-molecular weight transformation is applied, which determines the apparent molecular weight distribution. Since this distribution is highly sensitive to the relaxation frequencies of the molecules and aggregates, it clearly shows the interactions between the binder and the polymer and its shape may change considerably even if the oxidation does not significantly alter the real molecular weight. For this reason, the apparent molecular weight distribution represents an interesting means to quantify the effect of aging specifically in the case of polymer-modified binders.

## Data Availability

The raw data used to support the findings of this study are available from the corresponding author upon request.

## Conflicts of Interest

The authors declare that there is no conflict of interest regarding the publication of this paper.

## Acknowledgments

## References

[1] E. Prosperi and E. Bocci, "A review on bitumen aging and rejuvenation chemistry: processes, materials and analyses," *Sustainability*, vol. 13, no. 12, p. 6523, 2021.

[2] S. Filippi, M. Cappello, M. Merce, and G. Polacco, "Effect of nanoadditives on bitumen aging resistance: a critical review," *Journal of Nanomaterials*, vol. 2018, 17 pages, 2018.

[3] O. Sirin, D. K. Paul, and E. E. Kassem, "State of the art study on aging of asphalt mixtures and use of antioxidant additives," *Advances in Civil Engineering*, vol. 2018, 18 pages, 2018.

[4] G. D. Airey, "State of the art report on ageing test methods for bituminous pavement materials," *International Journal of Pavement Engineering*, vol. 4, no. 3, pp. 165–176, 2003.

[5] J. C. Petersen and E. R. Glaser, "Asphalt oxidation mechanisms and the role of oxidation products on age hardening revisited," *Road Materials and Pavement Design*, vol. 12, no. 4, pp. 795–819, 2011.

[6] Technical Activities Division, Transportation Research Board, e National Academies of Sciences, Engineering, and Medicine, *A Review of the Fundamentals of Asphalt Oxidation: Chemical, Physicochemical, Physical Property, and Durability Relationships*, no. article 23002, 2009Transportation Research Board, Washington, D.C., 2009.

[7] J. C. Petersen, "Quantitative method using differential infrared spectrometry for the determination of compound types absorbing in the carbonyl region in asphalts," *Analytical Chemistry*, vol. 47, no. 1, pp. 112–117, 1975.

[8] X. Lu and U. Isacsson, "Effect of ageing on bitumen chemistry and rheology," *Construction and Building Materials*, vol. 16, no. 1, pp. 15–22, 2002.

[9] M. le Guern, E. Chailleux, F. Farcas, S. Dreessen, and E. I. Mabille, "Physico-chemical analysis of five hard bitumens: Identification of chemical species and molecular organization before and after artificial aging," *Fuel*, vol. 89, no. 11, pp. 3330–3339, 2010.

[10] J. Xu, L. Sun, J. Pei, B. Xue, T. Liu, and E. R. Li, "Microstructural, chemical and rheological evaluation on oxidative aging effect of SBS polymer modified asphalt," *Construction and Building Materials*, vol. 267, article 121028, 2021.

[11] P. Marsac, N. Piérard, L. Porot et al., "Potential and limits of FTIR methods for reclaimed asphalt characterisation," *Materials and Structures*, vol. 47, no. 8, pp. 1273–1286, 2014.

[12] L. W. Corbett, "Composition of asphalt based on generic fractionation, using solvent deasphaltening, elution-adsorption chromatography, and densimetric characterization," *Analytical Chemistry*, vol. 41, no. 4, pp. 576–579, 1969.

[13] M. N. Siddiqui, M. F. Ali, and E. J. Shirokoff, "Use of X-ray diffraction in assessing the aging pattern of asphalt fractions," *Fuel*, vol. 81, no. 1, pp. 51–58, 2002.

[14] M. N. Siddiqui and E. M. F. Ali, "Investigation of chemical transformations by NMR and GPC during the laboratory aging of Arabian asphalt," *Fuel*, vol. 78, no. 12, pp. 1407–1416, 1999.

[15] J. C. Petersen, *Strategic Highway Research Program (U.S.), Binder Characterization and Evaluation*, vol. 1994, Strategic hirghway Research Program, National Research Council, Washington, D.C., 2020, Consultato: ott. 29: http://books.google.com/books?id=fypEqQY6lvAC.

[16] G. Polacco, S. Filippi, F. Merusi, and G. Stastna, "A review of the fundamentals of polymer-modified asphalts: asphalt/polymer interactions and principles of compatibility," *Advances in Colloid and Interface Science*, vol. 224, pp. 72–112, 2015.

[17] G. Airey, "Rheological properties of styrene butadiene styrene polymer modified road bitumens☆," *Fuel*, vol. 82, no. 14, pp. 1709–1719, 2003.

[18] L. Sun, Y. Wang, and E. Y. Zhang, "Aging mechanism and effective recycling ratio of SBS modified asphalt," *Construction and Building Materials*, vol. 70, pp. 26–35, 2014.

[19] X. Jin, R. Han, Y. Cui, and E. C. J. Glover, "Fast-rate–constant-rate oxidation kinetics model for asphalt binders," *Industrial & Engineering Chemistry Research*, vol. 50, no. 23, pp. 13373–13379, 2011.

[20] V. Mouillet, J. Lamontagne, F. Durrieu, J.-P. Planche, and L. Lapalu, "Infrared microscopy investigation of oxidation and phase evolution in bitumen modified with polymers," *Fuel*, vol. 87, no. 7, pp. 1270–1280, 2008.

[21] J. D. Ferry, *Viscoelastic properties of polymers, 3 rd*, Wiley, New York, 1980.

[22] W. H. Tuminello, "Molecular weight and molecular weight distribution from dynamic measurements of polymer melts," *Polymer Engineering and Science*, vol. 26, no. 19, pp. 1339–1347, 1986.

[23] W. H. Tuminello and N. Cudré-Mauroux, "Determining molecular weight distributions from viscosity versus shear rate flow curves," *Polymer Engineering and Science*, vol. 31, no. 20, pp. 1496–1507, 1991.

[24] L. Zanzotto, J. Stastna, and S. Ho, "Molecular weight distribution of regular asphalts from dynamic material functions," *Materials and Structures*, vol. 32, no. 3, pp. 224–229, 1999.

[25] L. Zanzotto, J. Stastna, and K. Ho, "Characterization of regular and modified bitumens via their complex modulus," *Journal of Applied Polymer Science*, vol. 59, no. 12, pp. 1897–1905.

[26] D. Yu, Y. Gu, and X. Yu, "Rheological-microstructural evaluations of the short and long-term aged asphalt binders through relaxation spectra determination," *Fuel*, vol. 265, article 116953, 2020.

[27] W. Thimm, C. Friedrich, M. Marth, and J. Honerkamp, "An analytical relation between relaxation time spectrum and molecular weight distribution," *Journal of Rheology*, vol. 43, no. 6, pp. 1663–1672, 1999.

[28] A. Gundla and B. Shane Underwood, "Molecular weight distribution of asphalt binders from laser desorption mass spectroscopy (LDMS) technique and its relationship to linear viscoelastic relaxation spectra," *Fuel*, vol. 262, article 116444, 2020.

[29] M. Jasso, J. Stastna, G. Polacco, and G. Cuciniello, "Development of internal structure of polymer-modified asphalts via transformations of the reduced frequency," *Journal of Applied Polymer Science*, vol. 138, no. 11, article 50037, 2021.

[30] D. Lesueur, A. Teixeira, M. M. Lázaro, D. Andaluz, and A. Ruiz, "A simple test method in order to assess the effect of mineral fillers on bitumen ageing," *Construction and Building Materials*, vol. 117, pp. 182–189, 2016.

[31] A. Themeli, E. Chailleux, F. Farcas, C. Chazallon, and B. Migault, "Molecular weight distribution of asphaltic paving binders from phase-angle measurements," *Road Materials and Pavement Design*, vol. 16, no. sup1, pp. 228–244, 2015.

[32] A. Themeli, E. Chailleux, F. Farcas, C. Chazallon, B. Migault, and N. Buisson, "Molecular structure evolution of asphaltite-modified bitumens during ageing; comparisons with equivalent petroleum bitumens," *International Journal of Pavement Research and Technology*, vol. 10, no. 1, pp. 75–83, 2017.

[33] K. Krolkral, S. Haddadi, and E. Chailleux, "Quantification of asphalt binder ageing from apparent molecular weight distributions using a new approximated analytical approach of the phase angle," *Road Materials and Pavement Design*, vol. 21, no. 4, pp. 1045–1060, 2020.

[34] G. Cuciniello, S. Filippi, M. Cappello, P. Leandri, and G. Polacco, "A revised relationship between molecular weight and reduced angular frequency in δ-method applied to unmodified petroleum bitumens," *Road Materials and Pavement Design*, p. 19, 2020.

[35] N. I. Yusoff, M. T. Shaw, and G. D. Airey, "Modelling the linear viscoelastic rheological properties of bituminous binders," *Construction and Building Materials*, vol. 25, no. 5, pp. 2171–2189, 2011.

[36] M. Yusoff and G. D. Airey, "The 2S2P1D: an excellent linear viscoelastic model," *Journal of Civil Engineering, Science and Technology*, vol. 1, no. 2, pp. 1–7, 2010.

[37] F. Olard and H. Di Benedetto, "General "2S2P1D" Model and relation between the linear viscoelastic behaviours of bituminous binders and mixes," *Road Materials and Pavement Design*, vol. 4, no. 2, pp. 185–224, 2003.

[38] C. Such, "Analyse du comportement visqueux des bitumes," *Bull Liaison Lab Ponts Chauss*, no. 127, pp. 23–35, 1983.

[39] S. Bhattacharjee, A. K. Swamy, and J. S. Daniel, "Continuous relaxation and retardation spectrum method for viscoelastic characterization of asphalt concrete," *Mechanics of Time-Dependent Materials*, vol. 16, no. 3, pp. 287–305, 2012.

[40] N. I. Yusoff, E. Chailleux, and G. D. Airey, "A comparative study of the influence of shift factor equations on master curve construction," *International Journal of Pavement Research and Technology*, vol. 4, no. 6, pp. 324–336, 2011.

[41] E. Chailleux, G. Ramond, C. Such, and C. de La Roche, "A mathematical-based master-curve construction method applied to complex modulus of bituminous materials," *Road Materials and Pavement Design*, vol. 7, no. sup1, pp. 75–92, 2006.

[42] G. D. Airey, "Use of Black diagrams to identify inconsistencies in rheological data," *Road Materials and Pavement Design*, vol. 3, no. 4, pp. 403–424, 2002.

[43] G. Cuciniello, P. Leandri, G. Polacco, G. Airey, and M. Losa, "Applicability of time-temperature superposition or laboratory-aged neat and SBS-modified bitumens," *Construction and Building Materials*, vol. 263, article 120964, 2020.

[44] Y. He, Z. Cao, Z. Liu, J. Li, J. Yu, and Y. Ge, "Influence of heat and ultraviolet aging on the structure and properties of high dosage SBS modified bitumen for waterproof," *Construction and Building Materials*, vol. 287, article 122986, 2021.

[45] V. Mouillet, F. Farcas, and S. Besson, "Ageing by UV radiation of an elastomer modified bitumen," *Fuel*, vol. 87, no. 12, pp. 2408–2419, 2008.

[46] G. Tarsi, A. Varveri, C. Lantieri, A. Scarpas, and C. Sangiorgi, "Effects of different aging methods on chemical and rheological properties of bitumen," *Journal of Materials in Civil Engineering*, vol. 30, no. 3, article 04018009, 2018.

[47] B. Hofko and M. Hospodka, "Rolling thin film oven test and pressure aging vessel conditioning Parameters: Effect on Viscoelastic Behavior and Binder Performance Grade," *Transportation Research Record*, vol. 2574, no. 1, pp. 111–116, 2016.

[48] J. Liu, J. Liu, and G. Hao, "Chemical aging indexes and rheological parameters for cracking susceptibility evaluation of Alaskan polymer–modified asphalt binders," *Journal of Materials in Civil Engineering*, vol. 33, no. 3, article 04021009, 2021.

[49] F. Wang, Y. Xiao, P. Cui, J. Lin, M. Li, and Z. Chen, "Correlation of asphalt performance indicators and aging degrees: a review," *Construction and Building Materials*, vol. 250, article 118824, 2020.

[50] N. Morian, C. Zhu, and E. Y. Hajj, "Rheological Indexes," *Transportation Research Record*, vol. 2505, no. 1, pp. 32–40, 2015.

[51] M. Cappello, G. Polacco, J. Crépier, Y. Hung, and S. Filippi, "Use of linear viscoelastic functions to estimate the aging resistance and internal structure of bituminous binders," *Applied Sciences*, vol. 11, no. 16, p. 7483, 2021.

[52] G. Cuciniello, P. Leandri, D. Lo Presti, M. Losa, and G. Airey, "Investigating the effect of artificial ageing on the creep and recovery of SBS-modified bitumen," *MATEC Web of Conferences*, vol. 271, article 03009, 2019.

[53] G. Cuciniello, P. Leandri, S. Filippi, D. Lo Presti, M. Losa, and G. Airey, "Effect of ageing on the morphology and creep and recovery of polymer-modified bitumens," *Materials and Structures*, vol. 51, no. 5, p. 136, 2018.

[54] C. S. Clopotel and H. U. Bahia, "Importance of elastic recovery in the DSR for binders and mastics," *Engineering Journal*, vol. 16, no. 4, pp. 99–106, 2012.

[55] Y. Ruan, "The effect of long-term oxidation on the rheological properties of polymer modified asphalts☆," *Fuel*, vol. 82, no. 14, pp. 1763–1773, 2003.

[56] K. Zhao, Y. Wang, L. Chen, and F. Li, "Diluting or dissolving? The use of relaxation spectrum to assess rejuvenation effects in asphalt recycling," *Construction and Building Materials*, vol. 188, pp. 143–152, 2018.

[57] K. Naderi, F. M. Nejad, and A. Khodaii, "Characterizing the aging of asphaltic materials through the evolution of continuous relaxation spectrum," *Petroleum Science and Technology*, vol. 37, no. 24, pp. 2404–2411, 2019.